



## Satellite mapping of emperor penguin habitat dispersal under climate extremes<sup>☆</sup>



Hong Lin <sup>a,b</sup>, Xiao Cheng <sup>a,b,\*</sup>, Jinyang Du <sup>c</sup>, John S. Kimball <sup>c</sup>, Ziyu Yan <sup>a,b</sup>, Teng Li <sup>a,b</sup>, Tongwen Li <sup>a</sup>, Yibo Li <sup>a,b</sup>, Zilong Chen <sup>a,b</sup>

<sup>a</sup> School of Geospatial Engineering and Science, Sun Yat-sen University, Southern Marine Science and Engineering Guangdong Laboratory (Zhuhai), Zhuhai 519082, China

<sup>b</sup> Key Laboratory of Comprehensive Observation of Polar Environment (Sun Yat-sen University), Ministry of Education, Zhuhai 519082, China

<sup>c</sup> Numerical Terradynamic Simulation Group, WA Franke College of Forestry and Conservation, University of Montana, Missoula, MT, USA

### ARTICLE INFO

#### Keywords:

Sustainable development goals  
Emperor penguin  
Habitat  
Extreme climatic events  
Antarctica  
Remote sensing

### ABSTRACT

Emperor penguins serve as early-warning sentinels for the Antarctic ecosystem and climate change. Understanding how climate change influences their habitat use offers insights into the fragile polar ecosystem for supporting the climate actions under the United Nations Sustainable Development Goals (SDGs). However, it remains unclear how the gradual climate change and extreme climatic events affect the dispersal of emperor penguin breeding habitats due to the lack of a systematic and long-term dataset documenting their habitat use. Here, we first develop guano indices and present an automated approach to map emperor penguin breeding habitats at 30-m spatial resolution using Earth observation satellite imagery, achieving a user accuracy of 94.8 %. We further reveal that habitat dispersal is sensitive to four extreme events—heat, blizzard, storm, and low sea ice. Specifically, colonies exposed to intense climate extremes generally exhibit more fragmented distributions, with habitat reuse periods mostly under 3 years and interannual habitat dispersal exceeding 4 km. These four extreme events together explained 21 %–72 % of the variability in annual habitat dispersal. Under a high-emission scenario driven by fossil fuels, the warming-induced annual fragmentation of habitats is projected to be 255 m greater than that under a low-emission scenario using clean energy, leading to higher vulnerability in emperor penguins by disrupting their ability to survive and reproduce. The proposed method enables routine mapping and updating of emperor penguin breeding habitats, and the associated findings demonstrate that extreme climatic events significantly impact habitat use and dispersal patterns, highlighting the urgent need for global climate policies aligned with sustainable development to protect the Antarctic ecosystem.

### 1. Introduction

Climate change and ecosystem degradation pose significant global challenges, and the United Nations Sustainable Development Goals (SDGs) provide a framework to address these issues (Hák et al., 2016). Specifically, Goal 13 (Climate Action), Goal 14 (Life Below Water), and Goal 15 (Life on Land) call for urgent action to mitigate climate impacts and protect biodiversity-rich ecosystems. Polar regions are critical in achieving global SDGs (Li et al., 2025). As top predators in the Antarctic ecosystem, emperor penguins (*Aptenodytes forsteri*) rely on stable sea ice as a breeding platform and are highly sensitive to environmental

changes (Barbraud and Weimerskirch, 2001), making them ideal sentinels for monitoring climate change and its ecological consequences. Evidence has shown that climate warming is increasing the survival pressure and extinction risk for emperor penguins (Jenouvrier et al., 2021; Jenouvrier et al., 2014; Trathan et al., 2020), and the International Union for Conservation of Nature (IUCN) has listed emperor penguins as a near-threatened species (IUCN, 2024). Utilizing satellite remote sensing for timely and large-scale mapping of emperor penguin habitats aligns with SDG 14 and SDG 15, as it provides essential datasets for assessing habitat degradation and informing conservation strategies. Quantifying the impacts of extreme climatic events on habitat use

<sup>☆</sup> This article is part of a Special issue entitled: 'SDGSAT-1 for SDGs' published in Remote Sensing of Environment.

\* Corresponding author. at: School of Geospatial Engineering and Science, Sun Yat-sen University, Southern Marine Science and Engineering Guangdong Laboratory (Zhuhai), Zhuhai 519082, China.

E-mail address: [chengxiao9@mail.sysu.edu.cn](mailto:chengxiao9@mail.sysu.edu.cn) (X. Cheng).

provides support for actions to mitigate the ecological consequences of climate change in Antarctica under SDG 13 (Labrousse et al., 2023; Trathan et al., 2011).

The dispersal behaviors of emperor penguins—including geographical shifts or permanent emigration—are key strategies for adapting to environmental changes (Forcada and Trathan, 2009). Efforts have been made to reveal the influence of ice conditions on habitat stability using remote sensing technology. For instance, declining sea-ice duration causes habitat loss (Trathan et al., 2011). Delayed fast-ice formation (Fretwell et al., 2014) and ice-tongue collapse (LaRue et al., 2015) force breeding-site relocation. Iceberg collision (Kooyman et al., 2007) and premature fast-ice breakup (Fretwell et al., 2023) lead to habitat destruction and breeding failure. However, a systematic description of emperor penguin habitat use over multiple years remains limited, and it is still unclear how extreme climatic events impact dispersal of emperor penguin breeding habitats in addition to the ice conditions. Unfortunately, with climate extremes projected to intensify in the future (Pörtner and Roberts, 2022), emperor penguin habitats are expected to be increasingly affected.

Here, we developed a method to map the breeding habitat use of emperor penguins at 30-m spatial resolution, and determined the sensitivity of habitat dispersal to environmental stability and extreme

climatic events, including anomalous heat, blizzard, storm, and low sea ice conditions. This study focuses on penguin dispersal as short-range movements within a breeding colony rather than long-range migration between different breeding colonies. We selected 10 important emperor penguin colonies representing four distinct habitat types (Labrousse et al., 2023), encompassing differences in population size, geographic characteristics, trophic competition, and physical characteristics (Fig. 1). We analyzed the habitat use patterns from 2013 to 2023 and conducted analyses from two temporal perspectives: (1) how environmental stability and mean intensity of extremes affect interannual dispersal and habitat use patterns, and (2) how annual habitat dispersal distance responds to anomalous heat, blizzard, storm, and low sea ice events.

## 2. Study area and data

### 2.1. Studied emperor penguin colonies

We selected 10 emperor penguin colonies for this study, with populations ranging from approximately 1000 to 26,000 individuals (Fig. 1). These colonies include some of the largest penguin populations, such as Coulman Island, Cape Colbeck, and Cape Washington, as well as

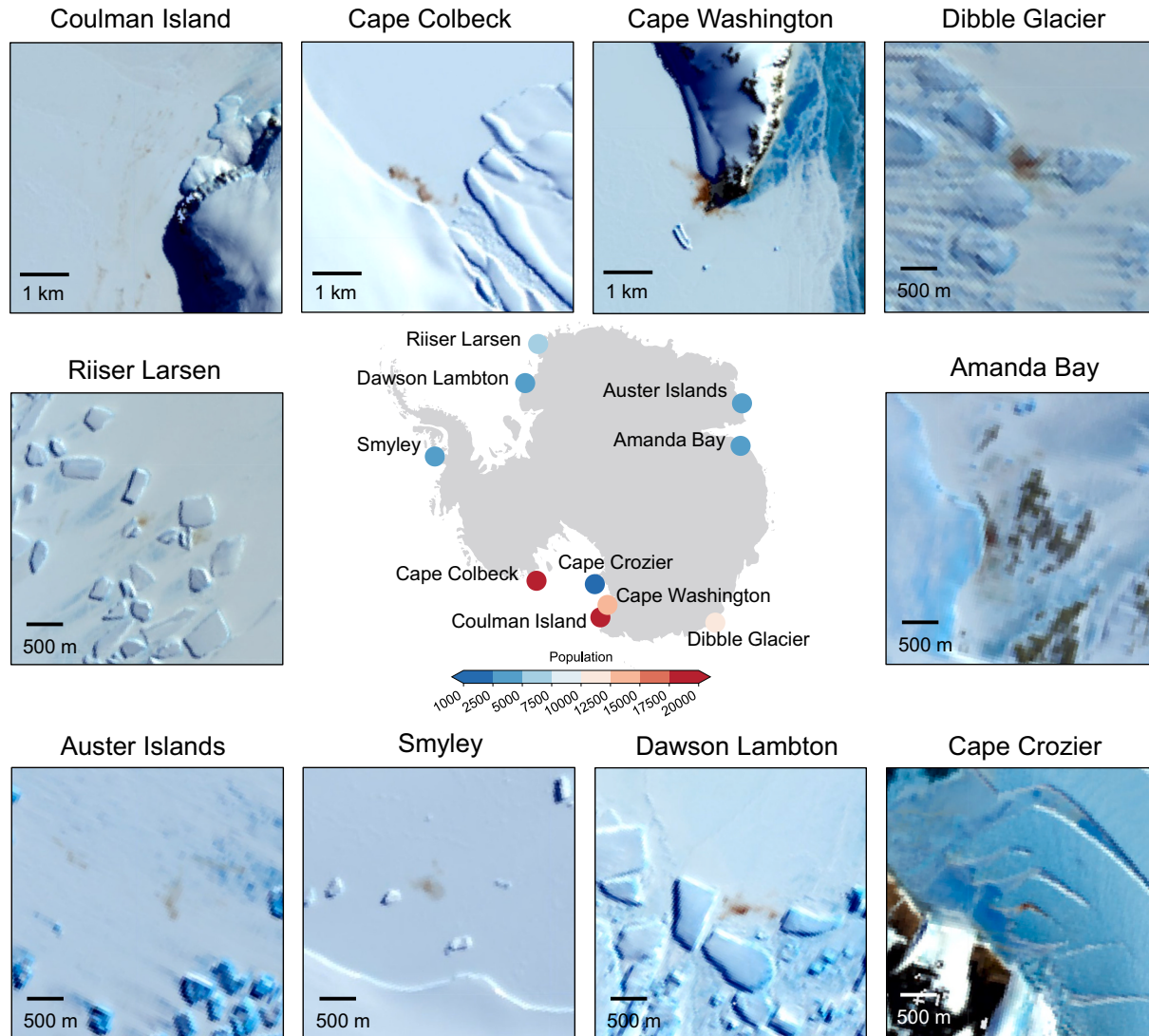


**Fig. 1.** Locations and populations of the studied colonies. The Landsat 8 OLI false colour image in the NIR-red-blue mode shows the distribution of penguin guano (indicated as darker shades overlying fast ice) across the 10 colonies. Penguin population was calculated based on the median number of adults. The maps use the Pseudo-Mercator projection. (For interpretation of the references to colour in this figure legend, the reader is referred to the web version of this article.)

medium-sized colonies and smaller ones like Cape Crozier. The locations of these colonies can be found in Table S1. The population data were collected from the Mapping Application for Penguin Populations and Projected Dynamics (MAPPPD) data record (Humphries et al., 2017) and from LaRue et al. (2024). These habitats encompass diverse geomorphological features and population sizes. For instance, both Coulman Island and Amanda Bay are located near rock outcrops, but Coulman Island lies within a vast fast-ice area, whereas Amanda Bay is situated in a relatively confined space (Fig. 1). This diversity allows our analysis to account for a wide range of scenarios. A previous study suggests that individual emperor penguins may not deviate from the population mean response due to Antarctica's extreme environment and strong selective pressures (Lescroël et al., 2014). Moreover, emperor penguins exhibit a homogeneous gene pool structure, indicating that the species may follow a shared evolutionary trajectory in response to environmental changes (Cristofari et al., 2016).

## 2.2. Landsat 8 imagery

The Landsat 8 satellite has a revisit cycle of 16 days, but it offers higher coverage frequency in the polar regions. We used images from this satellite mission that cover the studied colonies between September and November each year from 2013 to 2023, to detect emperor penguin guano as a proxy for habitat occupancy. We selected Landsat OLI (Operational Land Imager) surface reflectance data from the blue, green, red, near-infrared (NIR), and two shortwave infrared (SWIR) bands, all at a 30-m resolution. Images with cloud cover exceeding 50 % were excluded, and we used the pixel quality band to mask cloud, cloud shadow and water pixels for the remaining images. Pixels with red band values greater than 1.3 were masked to remove overly bright cloud tops and snow. We further used a rock distribution map (Burton-Johnson et al., 2016) to exclude rocky pixels. The above image preprocessing was performed in Google Earth Engine (GEE). Table S2 provides the timestamps of the Landsat 8 scenes used in this study.

## 2.3. Climate data

The surface skin temperature, snowfall, and wind speed data used in this study were obtained from the European Centre for Medium-Range Weather Forecasts Reanalysis 5 Land (ERA5-Land) dataset (Muñoz-Sabater et al., 2021). We used the daily ERA5-Land product, with a spatial resolution of 0.1°. Sea ice concentration (SIC) data were sourced from the AVHRR Pathfinder Version 5.3 Sea Surface Temperature (PFV53) dataset (Saha et al., 2018), which provides twice-daily observations (day and night) at 4-km spatial resolution. The SIC data in PFV53 were produced by the EUMETSAT Ocean and Sea Ice Satellite Application Facility (OSI SAF). We processed these datasets in GEE. The climate data used in this study correspond to the same period as the Landsat 8 imagery, specifically from September to November for each year between 2013 and 2023. These climate data were subsequently used to measure the intensity of extreme climatic events (Table S3, Section 3.5).

## 3. Methods

### 3.1. Guano indices

Guano stains left on fast ice by emperor penguins indicate the distribution of breeding habitats (Fretwell et al., 2012; Fretwell and Trathan, 2009). In addition, guano detected from remote sensing imagery has also been successfully used to detect other bird colonies. For example, Affine Transformation Classification has been applied to map Adélie penguin colonies (Schwaller et al., 2013), and the Spectral Angle Mapper has been used to detect unknown seabird colonies (Fretwell et al., 2015). However, there is a lack of established methods specifically designed for detecting emperor penguin guano in long-term satellite optical-infrared imagery. Large emperor penguin colonies generally

exhibit sufficiently strong guano signals on Landsat 8 satellite imagery to be detected, but identifying smaller colonies based solely on spectral band information poses greater challenges. This issue becomes particularly pronounced when a single classifier is applied to long-term and circum-Antarctic habitat detection with varying colony sizes. To effectively enhance the contrast between guano signals and the background, particularly for weak guano signals, we designed two guano indices based on the spectral characteristics of emperor penguin guano (Fig. 2a):

$$\begin{aligned} \text{Guano index 1} = & \frac{10(\text{NIR} - \text{Green})}{\text{NIR} + \text{Green} + 0.1} + \frac{\text{NIR} - \text{SWIR1}}{\text{NIR} + \text{SWIR1}} \\ & + \frac{\text{Red} - \text{Blue}}{\text{Red} + \text{Blue} + 0.01} + \frac{10(\text{SWIR1} - \text{SWIR2})}{\text{SWIR1} + \text{SWIR2} + 0.1} \end{aligned} \quad (1)$$

$$\text{Guano index 2} = \frac{(\text{SWIR1} - \text{SWIR2}) + 1.5(\text{NIR} - \text{Green})}{2(\text{SWIR1} + \text{SWIR2}) + 0.5} \quad (2)$$

where Red, Green, Blue, NIR, SWIR1, and SWIR2 represent the red, green, blue, near-infrared, and two shortwave infrared bands of Landsat 8 OLI imagery, respectively.

We take Cape Washington as an example to illustrate the typical spectral curves of guano and background samples, as well as their distribution in the guano indices (Fig. 3). Moreover, we conducted a more extensive evaluation—we collected 7960 guano pixels, 1575 rock pixels, and 6613 ice and snow pixels from Landsat 8 images across 23 emperor penguin colonies in Antarctica (Fig. S1a). These samples were independently collected by three trained image interpreters, with efforts made during the sampling process to include guano with a wide range of colour variations. All samples were subsequently reviewed by an experienced analyst. These sample points were collected across multiple years and encompassed a broad spectrum of guano signal intensities, represented by varying pixel colors from dark (indicating high guano concentration) to light (indicating low guano concentration) colors. We describe the development of the guano indices in more detail in the Supplementary Materials.

### 3.2. Image composition

To obtain the maximum habitat extent, we used a quality composite method to combine multiple Landsat 8 images into a single composite image. Quality composite refers to compositing multiple images by using a specific band as a quality metric, where the quality band serves as a per-pixel ordering criterion. Specifically, for a given habitat and year, we collected preprocessed Landsat 8 images from September to November. We selected guano index 1 as the quality band to evaluate the intensity of the guano signal in each pixel. For a given pixel location, the value of the pixel with strong guano signal, along with all associated bands, was retained in the final composite image (Fig. 2b). Here, we set the threshold for strong guano signals as the 90th percentile of guano index 1 to ensure the algorithm's resistance to outliers. The compositing algorithm ranks the pixels at the same location but on different dates based on the value of guano index 1, and selects the pixel at the 90th percentile in the sequence or the one closest to that percentile. This compositing process ensured that only pixels with strong guano signals were retained in the final composite image. Therefore, the composite image represents the maximum guano extent during September to November, rather than the distribution observed on any single day (Fig. 4). The guano area in Fig. 4 was calculated from the guano-covered regions detected in individual or composite images by summing the areas of all pixels within these regions. For guano detection, please see Section 3.3.

### 3.3. Mapping breeding habitats

In this section, our objective was to map emperor penguin breeding habitats from September to November, referred to as the annual habitat.

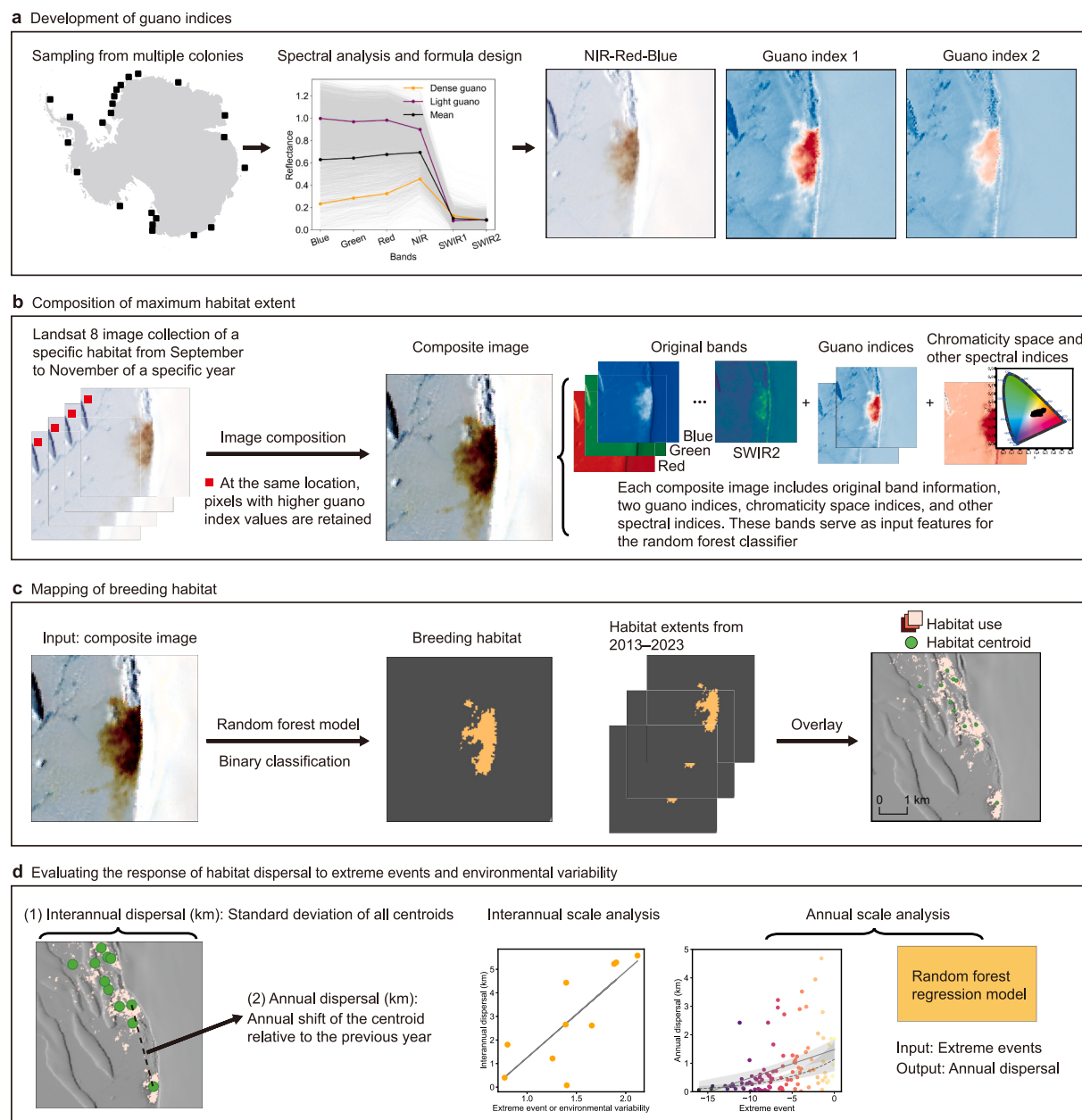


**Fig. 2.** Overview of the modeling process. a, Landsat 8 OLI imagery was used to collect samples across multiple Antarctic colonies, and guano indices were designed based on the spectral characteristics of emperor penguin guano. b, Multiple satellite images within the same breeding season were composited using guano index 1 as the quality standard. Composite images represent the maximum habitat extent from September to November. c, A random forest model performed binary classification on the composite images to determine the annual breeding habitat extent. Habitat use maps were derived by overlaying all annual habitat maps. d, Interannual and annual habitat dispersal were calculated. The relationships between interannual dispersal and two factors were analyzed: (1) the mean intensity of extreme events, calculated as the average of annual intensities from 2013 to 2023, and (2) environmental variability. Correlations between annual dispersal and extreme event intensities were examined. A habitat dispersal model driven by extreme events was developed using random forest regression.

We used a random forest machine learning model to detect penguin habitats (i.e., inferred from guano signals). Random forest is an ensemble learning algorithm that combines multiple decision trees to improve classification accuracy and stability (Breiman, 2001). It exhibits strong resistance to overfitting and is well-suited for handling a large number of features (Belgiu and Drăguț, 2016; Maxwell et al., 2018). The random forest model can further assess the importance of each feature and provide insights for feature selection in future habitat detection research. Our random forest model performed a binary classification at the pixel level (guano or non-guano).

Combining spectral indices with multiple spectral bands as predictors for classifiers has been demonstrated to be an effective approach

for target detection (Wang et al., 2023). For each satellite image, we calculated two guano indices, two International Commission on Illumination (CIE) colour space indices, and seven additional spectral indices (see Supplementary Materials). After image composition, each resulting image set includes six spectral bands (blue, green, red, NIR, SWIR1, and SWIR2), and 11 spectral indices, totaling 17 bands. Therefore, the model inputs were composite annual (Sep–Nov) images containing 17 predictors, and the model output was the habitat extent map for each year of record. We selected these predictors based on two main considerations: improving model performance and assessing the importance of each predictor in guano detection.

To train the random forest model, we collected 1989 guano sample

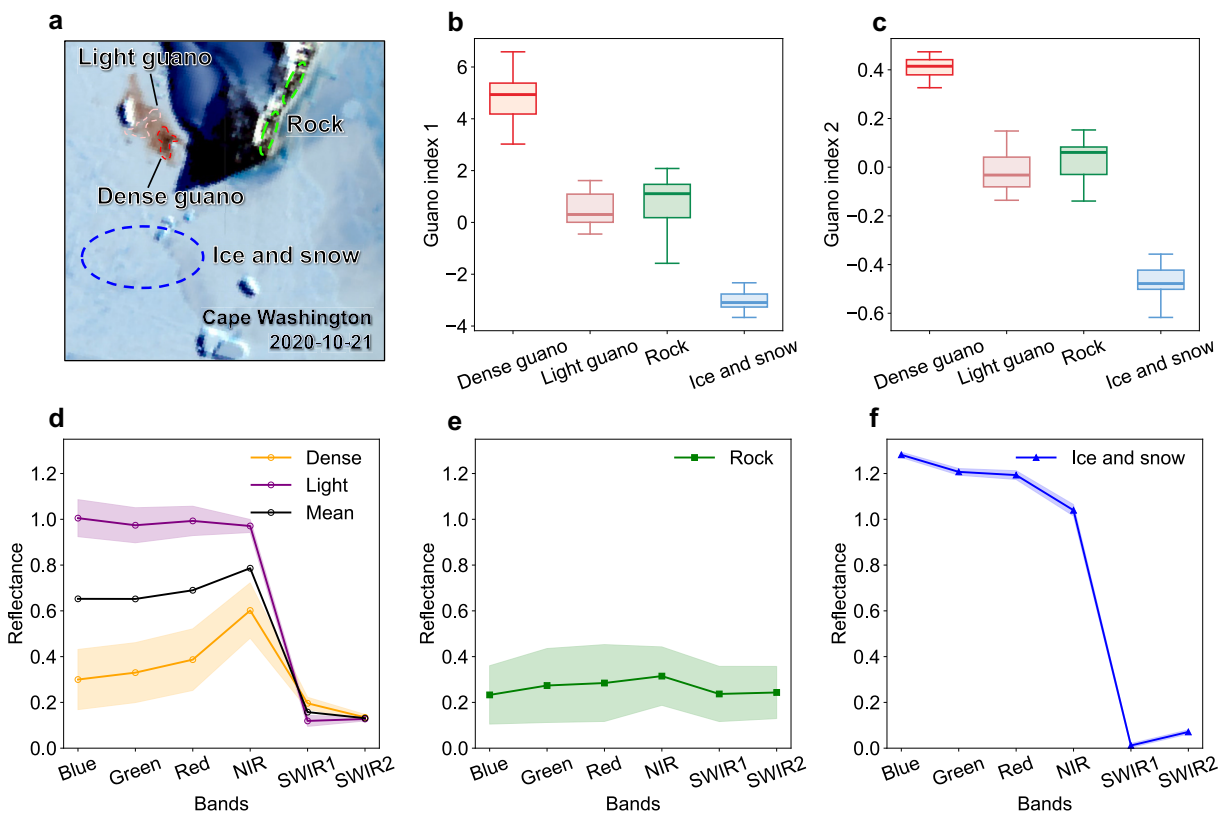


**Fig. 3.** Development of the two guano indices using Landsat satellite imagery. (a) Landsat 8 OLI false colour image shows dense guano, light guano, rocks, ice, and snow at Cape Washington. (b) and (c) show the value distribution for guano index 1 and guano index 2 of different surface features. (d) to (f) present the spectra of guano, rocks, ice, and snow, respectively. The shaded area represents  $\pm 1$  standard deviation.

points and 64,897 non-guano sample points from composite images spanning multiple years across the studied colonies. The total dataset was split into 80 % for training and 20 % for testing. During model training, we used grid search combined with a five-fold cross-validation approach to determine the model's hyperparameters (Table S4). Specifically, the training data were divided into five folds, with each fold being mutually exclusive. For a given set of hyperparameters, the model was trained and validated five times. In each iteration, one fold was used as the validation set while the remaining four served as the training set. The performance metrics from the five iterations were averaged for model evaluation. The final model was then tested on the test set to assess its performance. We selected user accuracy, producer accuracy, and the F1 score to evaluate the model's performance. User accuracy refers to the probability that a pixel classified as a certain category on the map truly belongs to that category. For users, it reflects the reliability of the map. Producer accuracy refers to the probability that a pixel which truly belongs to a certain category is correctly classified as that category on the map. For data producers, it indicates the extent of omission errors for that category.

We overlaid the annual habitat maps to generate habitat use maps for 2013–2023 and categorized habitat use into three types: less than 3 years, 3–6 years, and more than 7 years (Fig. 2c, Fig. 9). In addition, we plotted habitat use maps showing progressively increasing occupancy duration as a supplement (please see Fig. S2).

#### 3.4. Habitat dispersal

We calculated habitat centroids for the annual habitat maps and evaluated both interannual and annual dispersal patterns. For the interannual analysis, we calculated the standard deviation of centroid coordinates across the study period for a given habitat and converted it into distance (Fig. 2d). This distance served as a measure of the habitat's

interannual dispersal level. For the annual analysis, the distance between centroids in consecutive years was calculated to represent annual habitat dispersal. The shift in habitat centroids is not sensitive to local anomalous variations and reflects the overall dispersal trend.

#### 3.5. Extreme climatic events

We analyzed the effects of four extreme climatic events (heat, blizzard, storm, and low sea ice) on habitat dispersal. For a given habitat and year, the highest daily maximum skin temperature from September to November was used as the measure for heat, the total snowfall over the snowiest consecutive five days as the measure for blizzard, and the highest daily maximum wind speed as the measure for storm. These metrics referenced the framework of the Expert Team on Climate Change Detection and Indices (ETCCDI) (Sillmann et al., 2013). The minimum SIC during September to November was used as the measure for low sea ice. The period from September to November represents a critical breeding season for emperor penguins (Fig. S3) and coincides with the time when optical satellites can detect strong habitat signals (Winterl et al., 2024), aligning with the habitat mapping period in this study.

For heat, blizzard, and storm, the mean intensity within a 50-km radius of the habitat location was calculated, while for low sea ice, a 20-km radius was used. We tested different buffer sizes and found that the correlation between sea ice and habitat dispersal increased as the buffer area decreased, whereas the correlation between other variables and dispersal was not particularly sensitive to buffer size (Figs. S4 and S5). We used a percentile threshold method to assess extreme conditions of climate variables during the climatological period (1980–2014) and compared it with the intensity of extreme events during the study period. The results show that most extremes exhibited greater intensity compared to the extreme measures of the climatological period,

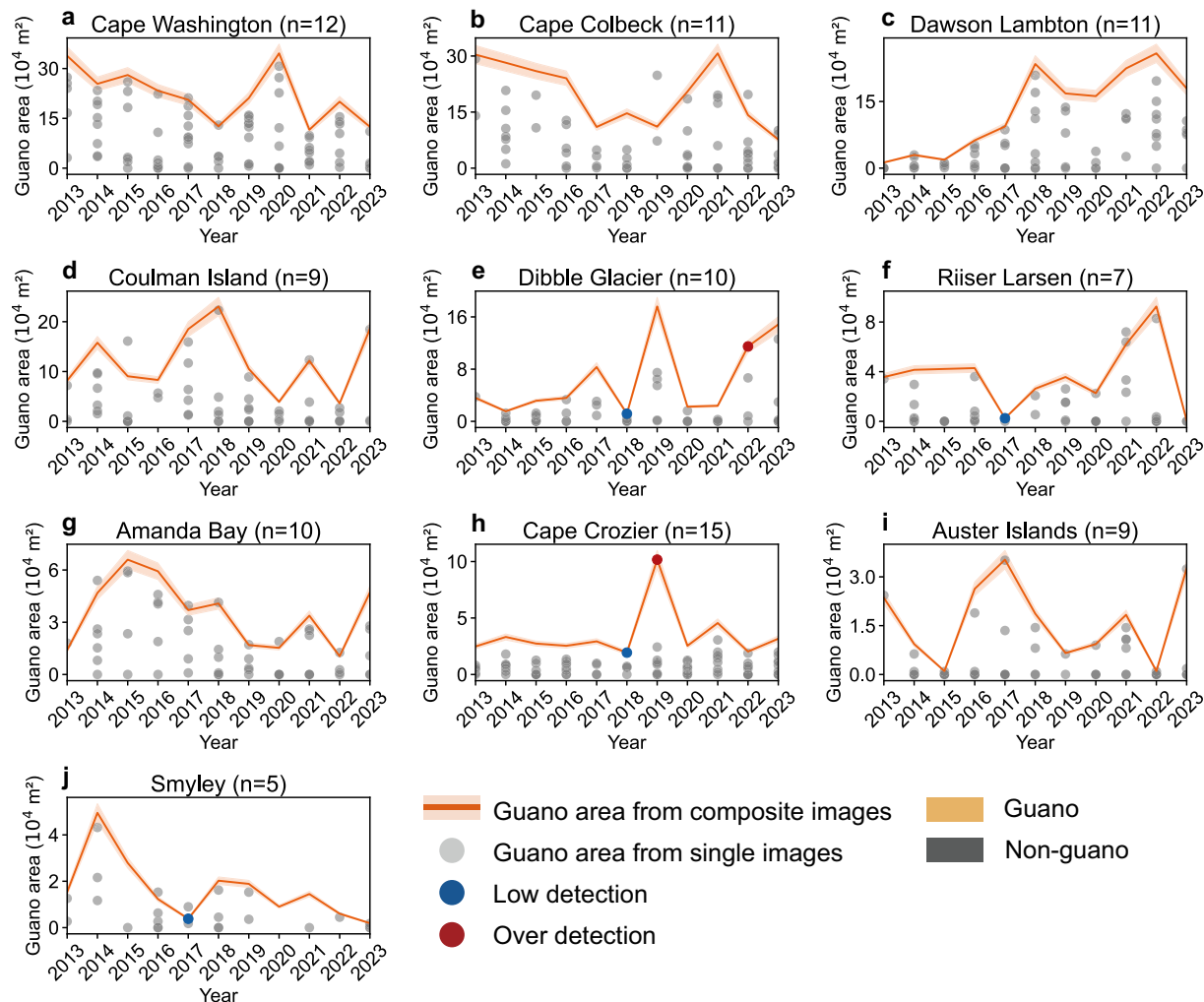


**Fig. 4.** Comparison of habitat extents detected from Landsat composite images and individual images within the same breeding season. a–j, The guano extents detected from composite images represent the potential habitat distribution during September to November (orange lines; shading indicates an 8 % uncertainty level in guano detection). In contrast, habitat extents detected from individual images exhibit high variability (grey dots; only results with cloud cover  $\leq 20\%$  are shown). Red and blue dots represent over detection and low detection, respectively, both indicating low detection quality. ‘n’ denotes the mean number of satellite images available per year for each habitat from September to November during 2013–2023 (cloud cover  $\leq 50\%$ ). k, An example from Coulman Island in 2014 illustrates that emperor penguin breeding colonies exhibit significant variability at different times within a breeding season, which is captured by the composite image. (For interpretation of the references to colour in this figure legend, the reader is referred to the web version of this article.)

indicating that they were not only extreme relative to the study period (Fig. 5). To evaluate habitat environmental variability, we calculated the mean values of skin temperature, snowfall, wind speed, and SIC from September to November for each habitat and determined the standard deviations of these variables from 2013 to 2023.

### 3.6. Correlation and response analysis

At the interannual scale, we calculated the correlation between interannual habitat dispersal and the mean intensity of extreme events from 2013 to 2023, as well as between interannual habitat dispersal and environmental fluctuation. Pearson correlation coefficients ( $R_p$ ) and Spearman correlation coefficients ( $R_s$ ) were used. At the annual scale,

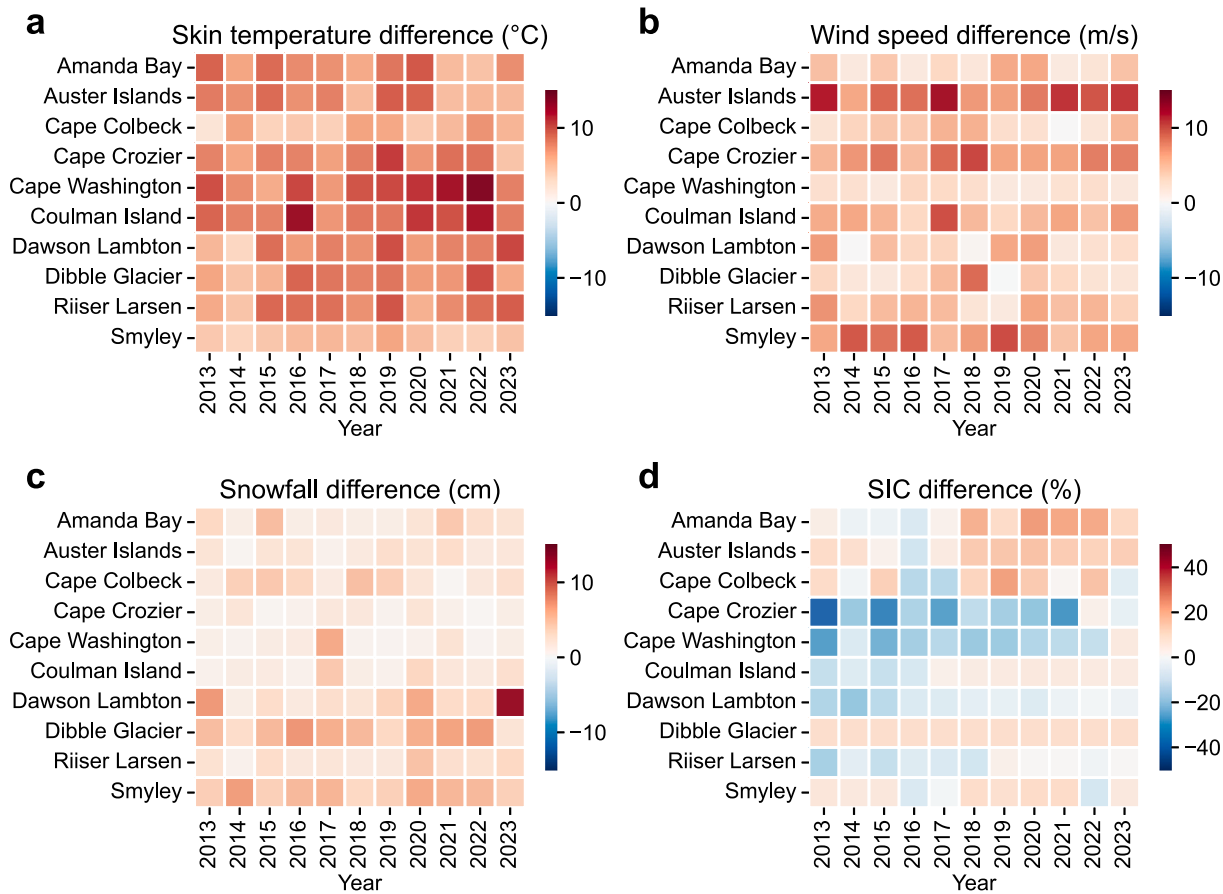


**Fig. 5.** Differences in extreme climatic event intensities during the study period (2013–2023) compared to thresholds from the climatological baseline (1980–2014). Each cell represents the intensity of an extreme event during September–November for a given habitat in a specific year, subtracted by the extreme event threshold from the baseline period. a–c, Thresholds for skin temperature (a), wind speed (b), and snowfall (c) during the baseline period were set at the 90th percentile of all September–November values from 1980 to 2014. d, The threshold for SIC during the baseline period was set at the 15th percentile of September–November values. Results show that, for most years during the study period, the intensities of extreme events exceeded the thresholds from the climatological baseline.

we calculated the  $R_s$  and  $R_p$  between annual habitat dispersal distance and the intensity of extreme climatic events in the same year. Linear regression and exponential regression were applied for curve fitting. To analyze the response of annual habitat dispersal to extreme climatic events of varying intensities, we divided the events into groups based on intensity levels and conducted a two-tailed permutation test to examine whether dispersal distance differed significantly between groups. The grouping thresholds for heat, blizzard, storm, and low sea ice were set at  $-5^{\circ}\text{C}$ , 5 cm, 10 m/s, and 80 %, respectively. We tested different thresholds and found that the significance of the grouping was not sensitive to the choice of thresholds (Fig. S6).

### 3.7. Habitat dispersal model

We developed a habitat dispersal model using annual habitat dispersal as the response variable and heat, blizzard, storm, and low sea ice as the predictors. The purpose of this model was not to perfectly predict emperor penguin habitat dispersal but to evaluate the comprehensive effects of extreme climatic events on habitat dispersal and quantify the response of habitat dispersal to individual events. This is because the factors affecting the quality of habitats mainly include climate, food availability, and safety (Budd, 1961). For emperor penguins, habitat safety includes the need to avoid predators such as sea lions, leopard seals, orcas, and predatory birds, as well as geomorphological features such as crevasses, avalanches, and icefalls. To fit the model, we selected random forest regression, an ensemble machine learning algorithm that integrates multiple decision trees to enhance

model stability and resistance to overfitting (Breiman, 2001). We tested several other algorithms, but random forest regression demonstrated the best predictive performance. The response variable showed a pronounced right-skewed distribution, with fewer data points at higher dispersal distance (Fig. 6). To address this, a square root transformation was applied to the response variable to reduce skewness (Bartlett, 1947) and enhance model learning performance (Osborne, 2010). Consequently, the input response variable for the random forest regression model was the square root of annual dispersal distance, but all final predictions were transformed back to the original scale. Accuracy evaluation was also conducted on the original scale of the predictions.

We used a bootstrap method to assess model performance. Specifically, the data were randomly split, with 80 % for training and 20 % for testing. For model training, hyperparameters were determined using 5-fold cross-validation. The final model for each data split was evaluated on the test set using the coefficient of determination ( $R^2$ ) and root mean squared error (RMSE) as performance metrics. This entire process—from data splitting to model evaluation—was repeated 10 times. The mean  $R^2$  and mean RMSE from the 10 repetitions were used as the overall evaluation of model performance, while the mean importance of predictors across the 10 iterations was used to assess the importance of extreme climatic events. The response of annual habitat dispersal to individual extreme events was derived from the trained random forest model by varying only the variable of interest, while keeping other covariates constant.

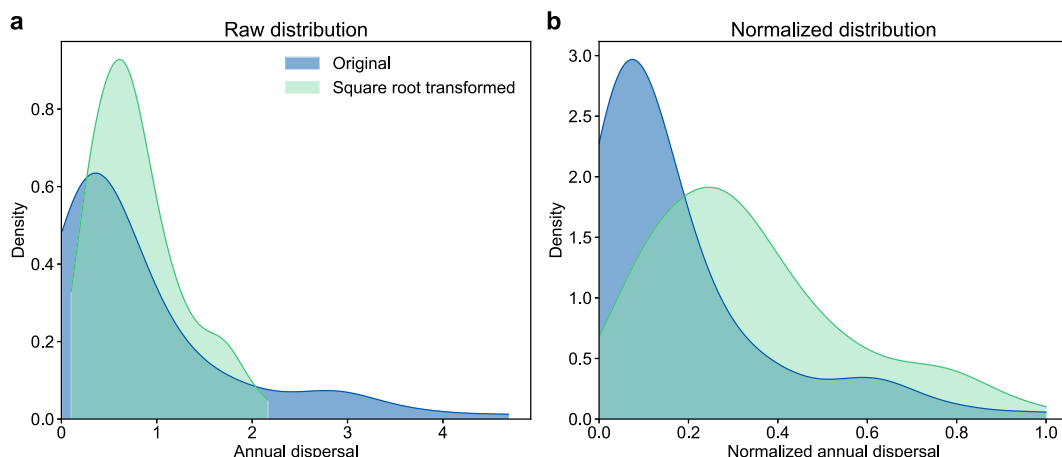


**Fig. 6.** Comparison of the distributions of the original response variable (blue) and the square-root-transformed response variable (green) on their raw scales (a) and on the normalized scales (b). (For interpretation of the references to colour in this figure legend, the reader is referred to the web version of this article.)

## 4. Results

### 4.1. Performance of habitat mapping

Our best random forest classification model achieved a user accuracy of 94.8 %, a producer accuracy of 83.4 %, and an F1 score of 0.89. Through visual inspection of the habitat detection results, we generated a quality label for each habitat map (Fig. 7a). Overall, our method achieved an acceptance rate of 90 %. Among these, 99 were classified as acceptable normal detection, three as low detection, two as over detection, and an additional six were marked as low image quality due to extensive cloud contamination. The three low detection images exhibited weak guano signals, such as in Auster Islands in 2022 (Fig. 7b).

We attributed these low detection results to our methods' limitation in detecting very weak guano signals. Terrain shadowing did not constrain our habitat detection (Fig. S7, Cape Colbeck, Riiser Larsen, and Dawson Lambton).

The guano indices were identified as the best features for habitat detection in our model, with a total importance of 31.7 % (Table S5). Fig. 8 demonstrates the effectiveness of the guano indices in delineating guano contours. We performed a two-tailed permutation test on guano index 1 and guano index 2 for guano, rock, and ice-snow samples from 23 emperor penguin colonies and found that both guano indices differed significantly from those of the background ( $P < 0.001$ ). Note that in this evaluation, both guano and rock samples included very weak-signal samples (Fig. S1) to assess the performance of the guano indices under

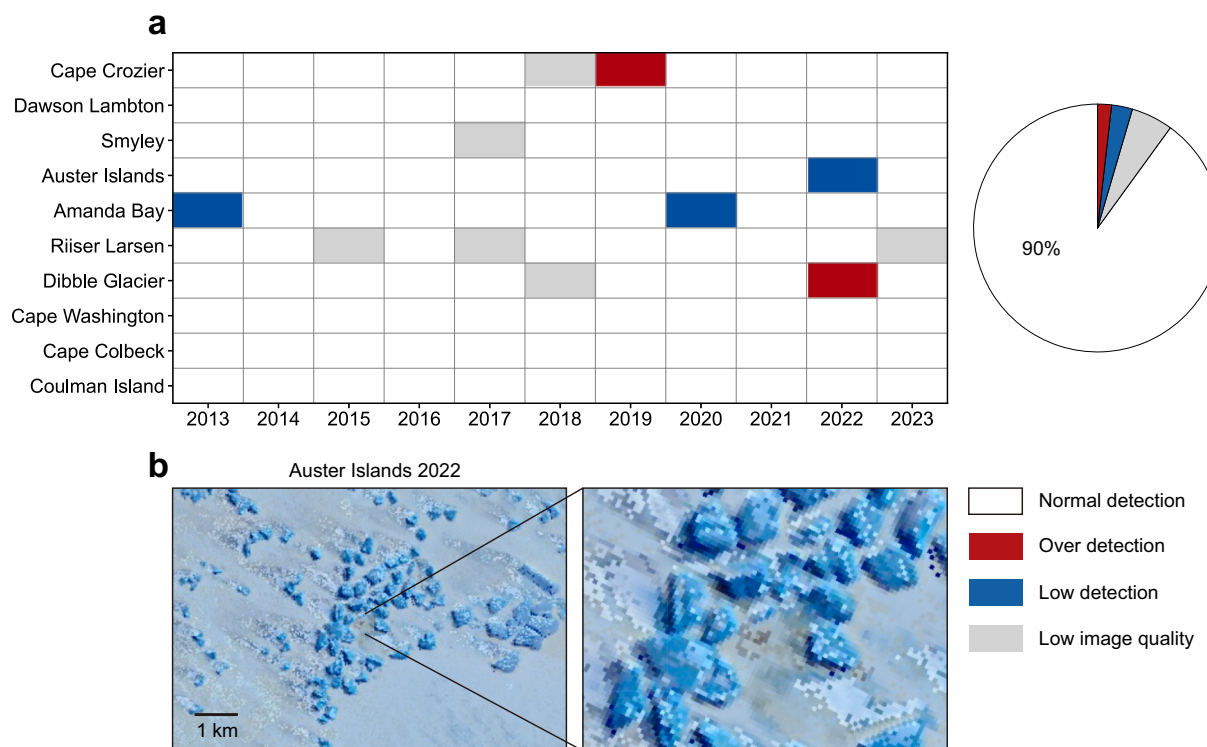


**Fig. 7.** Performance of the habitat detection algorithm. (a) Quality assessment of the habitat detection results, including labels for acceptable normal detection (white grids), over detection (red grids), low detection (blue grids), and low image quality (grey grids). (b) An example of low detection is provided by the composite image of Auster Islands in 2022, where the guano signal is weak. (For interpretation of the references to colour in this figure legend, the reader is referred to the web version of this article.)

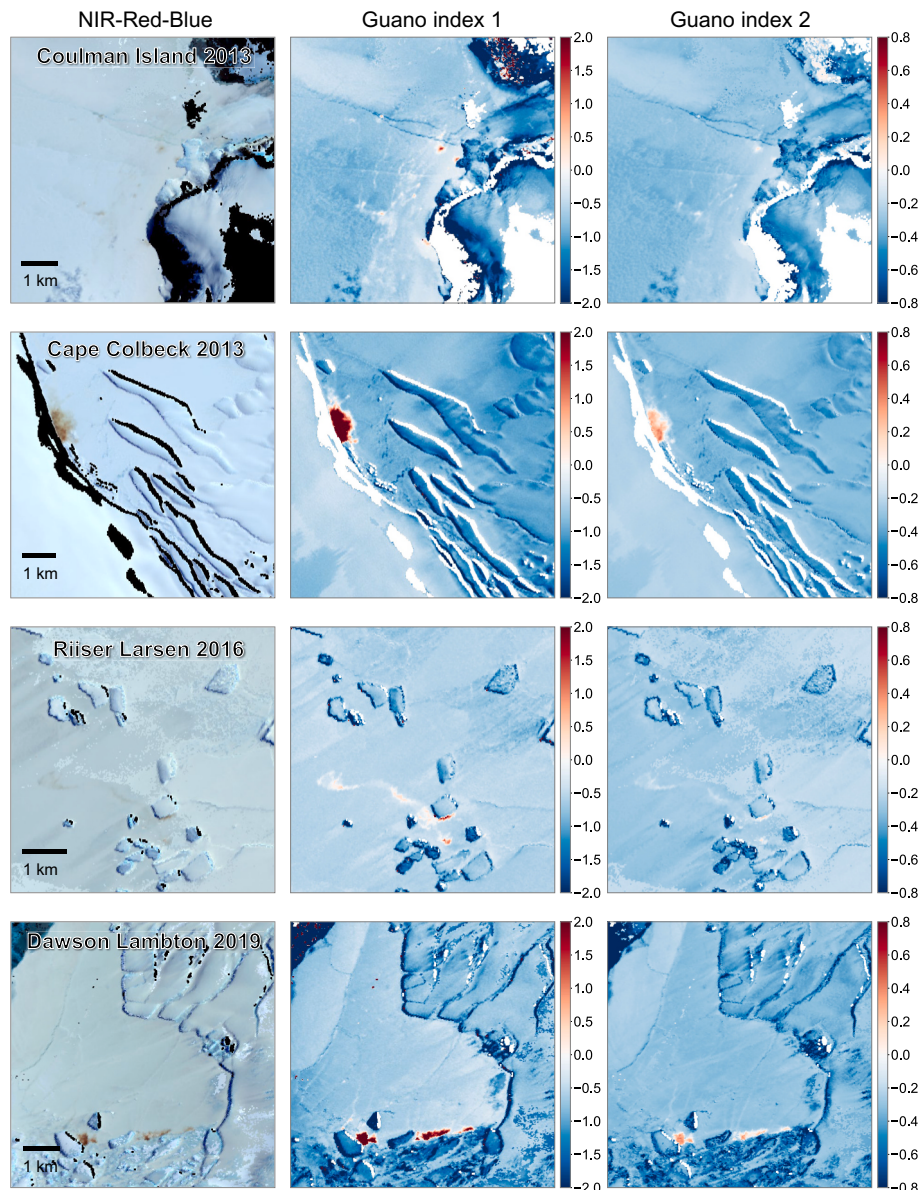


**Fig. 8.** Performance of the two guano index maps in four selected colonies. These guano index maps were generated from composite images. Performance of the guano indices in more emperor penguin colonies can be found in Fig. S7.

stringent conditions. For typical guano spectral curves, refer to Fig. 3.

#### 4.2. Habitat use and interannual dispersal

The studied habitats are distributed in areas near rock outcrops, ice cliffs, or icebergs (Fig. 9). Emperor penguins prefer these relatively stable and sheltered locations (Kooyman, 1993). For example, the terrain at Coulman Island shields against prevailing southeast winds (Budd, 1961), and wind speeds tend to be lower near Cape Washington. Grounded icebergs not only provide shelter but also help anchor fast ice, enhancing its stability (Budd, 1961). The habitats at Riiser Larsen and Auster Islands are located within such grounded iceberg chains (Fig. 9f, h). Moreover, icebergs, islands and ice tongues facilitate the formation of tidal cracks, providing foraging grounds for emperor penguins (Budd, 1961). Cape Washington, Coulman Island, and Amanda Bay exhibit longer habitat reuse duration (Fig. 9b,d,g, Fig. 10). Habitats with long reuse duration may indicate areas of significant biological advantages, as emperor penguins need to balance climatic conditions, food availability, and habitat safety (Budd, 1961). Indeed, Cape Washington,

Coulman Island, and Amanda Bay feature stable fast ice and favorable ocean access (Budd, 1961). Cape Washington and Coulman Island are also among the world's largest emperor penguin colonies.

We found a positive correlation between interannual habitat dispersal and the mean intensity of extreme climatic events, with  $R_p$  ranging from 0.48 to 0.67 (Fig. 11a–c). Colonies exposed to more intense heat, blizzard, and storm events, such as Dibble Glacier, Auster Islands, and Smyley (Fig. 9e,h,i), typically exhibited more fragmented habitat distribution. These habitats experienced interannual dispersal exceeding 4 km and reuse duration of less than 3 years during 2013–2023 (Fig. 10). In contrast, colonies with lower mean intensities of extremes, such as Cape Washington, exhibited more concentrated habitat distribution, with interannual dispersal of 0.4 km and reuse duration exceeding 7 years. The SIC around habitats reflects both fast and pack ice conditions, indicating habitat stability and food availability (Croxall et al., 2002). Emperor penguins need to compromise on these factors. For example, Cape Crozier's ice is less stable, but the nearby open waters along the Ross Ice Shelf provide good foraging opportunities (Budd, 1962). During the study period, the intensities of extreme weather were comparable for

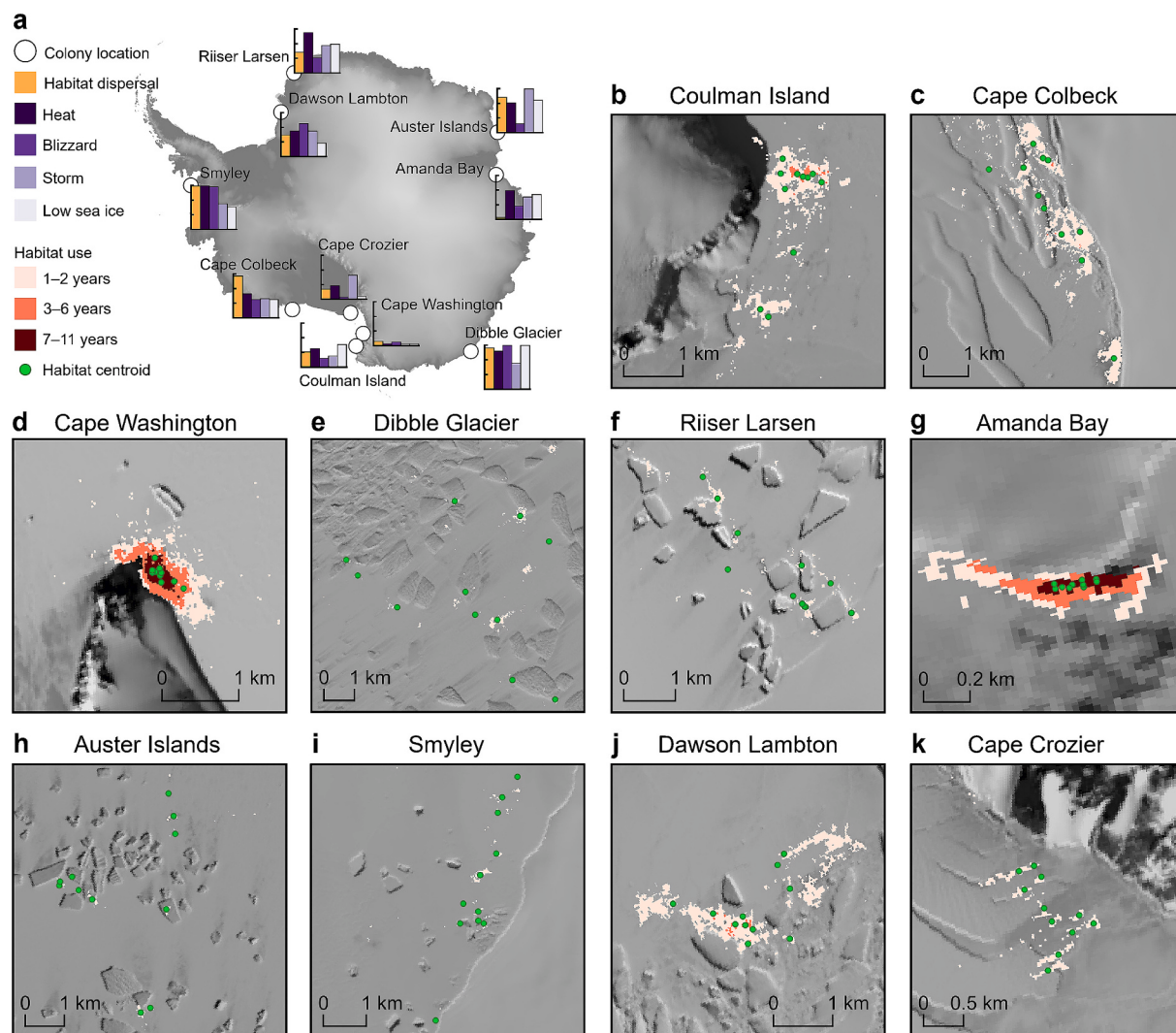


**Fig. 9.** Emperor penguin breeding habitat use, interannual dispersal, and extreme climatic events between 2013 and 2023. a, Bar charts show the interannual habitat dispersal and the mean intensities of heat, blizzard, storm, and low sea ice events of the studied colonies (white circles). All variables are normalized. b–k, Patterns of breeding habitat use and annual habitat centroids (green dots). (For interpretation of the references to colour in this figure legend, the reader is referred to the web version of this article.)

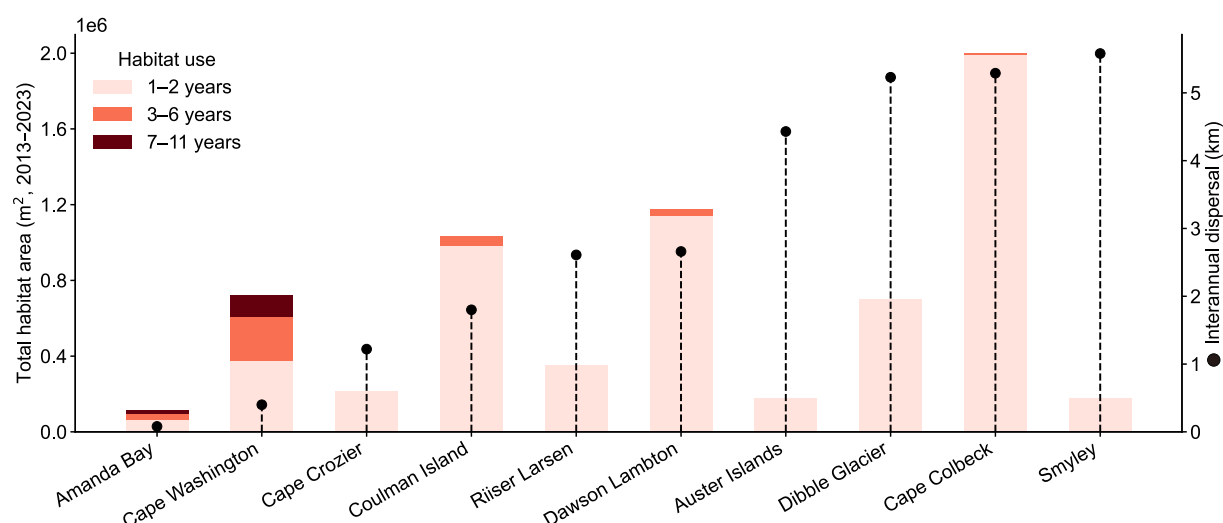


**Fig. 10.** Habitat use and interannual dispersal of the studied emperor penguin colonies from 2013 to 2023. The bar chart shows the habitat area categorized by different durations of use. Black dots represent interannual habitat dispersal, calculated as the standard deviation of habitat centroids across all years.

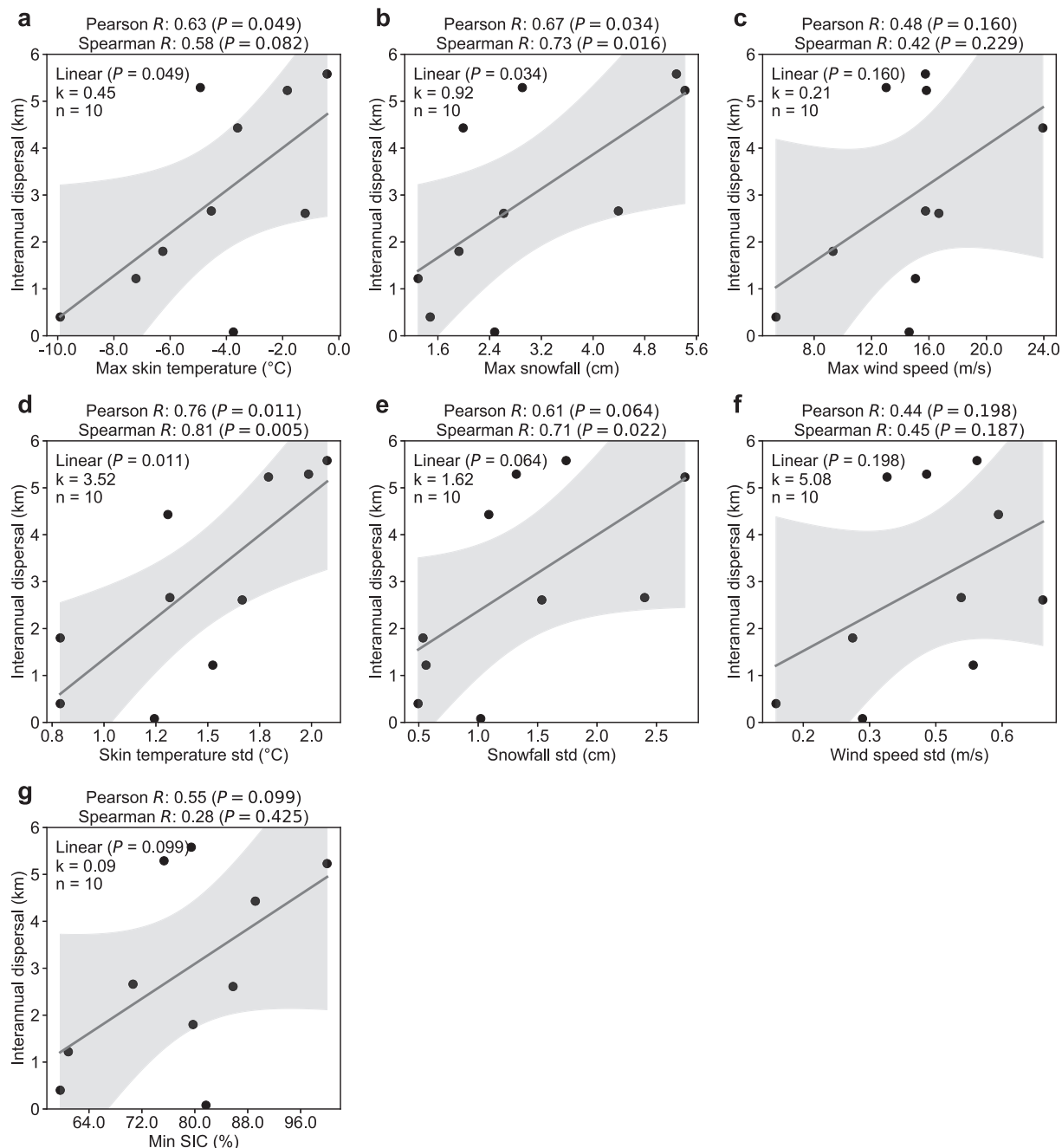


**Fig. 11.** Interannual habitat dispersal and environmental variability. a–c, Correlation between interannual dispersal and the mean intensity of extreme events, including heat (a), blizzard (b), and storm (c). d–f, Correlation between interannual dispersal and environmental variability. Environmental variability was assessed by calculating the standard deviation of the mean values for skin temperature (d), snowfall (e), and wind speed (f) during September–November between 2013 and 2023. g, Correlation between the interannual mean of minimum SIC and interannual dispersal. Pearson and Spearman correlation coefficients are annotated in each panel. Data were fitted using linear regression, with model significance ( $P$ ) and slope ( $k$ ) indicated.

Cape Colbeck and Amanda Bay, but Cape Colbeck showed a higher interannual dispersal level (Fig. 9, Fig. 10). This may be attributed to geographic factors—Cape Colbeck is within extensive fast ice, offering greater dispersal space but also exposing the colony to more open environments. In contrast, Amanda Bay is sheltered by tall ice cliffs upwind and multiple islands downwind. This topography limits available space but creates a stable microclimate with reduced wind speeds within the habitat (Budd, 1961). Therefore, under similar climatic pressures, the geomorphological features of habitats may play a critical role in shaping emperor penguins' long-term dispersal patterns.

Environmental instability also contributes to habitat dispersal. Fluctuations in surface skin temperature, snowfall, and wind speed are

positively correlated with interannual habitat dispersal, with  $R_p$  ranging from 0.44 to 0.76 (Fig. 11d–f). This suggests that environmental fluctuations may drive emperor penguins to move between years in search of more suitable breeding sites. These patterns are supported by the following: (i) emperor penguins do not build nests, allowing for greater mobility (Kooyman and Ponganis, 2017). (ii) previous studies on ice conditions show that emperor penguins migrate in response to unstable environments, including short-range movements (Fretwell et al., 2014; Trathan et al., 2011).

#### 4.3. Response of annual habitat dispersal to extreme events

Overall, there was a significant positive correlation ( $P < 0.05$ ) between extreme event intensity and annual habitat dispersal distance, with  $R_p$  ranging from 0.26 to 0.43 and  $R_s$  ranging from 0.27 to 0.45 (Fig. 12). This positive trend aligns with observations of increased dispersal rates in Adélie penguins (*Pygoscelis adeliae*) under harsh environmental conditions (Dugger et al., 2010). We further identified significant differences ( $P < 0.05$ ) in the responses of annual habitat dispersal distance to varying intensities of extreme events (Fig. 13). Specifically, when the maximum daily skin temperature exceeded  $-5^{\circ}\text{C}$ , the mean dispersal distance was 1.13 km, which is 2.6 times the value observed when the temperature was below  $-5^{\circ}\text{C}$  (0.43 km; Fig. 13a). Similarly, when the maximum total snowfall exceeded 5 cm, the mean annual dispersal distance was 1.57 km—2.2 times that under snowfall below 5 cm (0.71 km; Fig. 13c). These findings indicate that emperor penguins tend to move greater distances in search of more suitable breeding sites as the intensity of extreme events increases.

To analyze the comprehensive effect of extreme events on annual habitat dispersal and quantify the sensitivity of dispersal distance to each covariate, we constructed a habitat dispersal model driven by extreme events. We found that heat, blizzard, storm, and low sea ice collectively explained 21 % to 72 % of the variance in annual habitat dispersal, with a mean explanatory power of 40 % (Fig. 14a). By holding other variables constant, we isolated the response curves of annual dispersal distance to each climatic predictor (Fig. 14c–f). Skin temperature and snowfall were identified as the most important predictors in the habitat dispersal model (Fig. 14b), and annual dispersal showed greater sensitivity to these two factors (Fig. 14c, e). Specifically, for every  $1^{\circ}\text{C}$  rise in skin temperature, the annual habitat dispersal distance increased by 73 m (95 % confidence interval (CI): 68–79 m). A rise of 1 cm in snowfall corresponded to an increase of 66 m in annual dispersal (95 % CI: 60–71 m). The effects of wind speed and SIC on annual dispersal were non-monotonic—dispersal distance increased when these variables were either very low or very high (Fig. 14d,f).

## 5. Discussion

### 5.1. Contributions and innovations

This study provides a novel method for detecting emperor penguin habitats based on Landsat satellite imagery, enabling routine mapping of circumpolar emperor penguin habitat distribution and updates on habitat use. Compared to previous studies that relied on manual annotation of habitat locations and visual interpretation of habitat shifts, the proposed approach is more automated and efficient. Moreover, this study introduces two new satellite-based guano indices as effective tools in mapping emperor penguin guano from background conditions, which can be further explored by the scientific community, such as for

identifying and monitoring potential habitats. This study also reveals the significant impacts of extreme climatic events on the patterns of emperor penguin breeding habitat use and dispersal. Habitats exposed to substantial environmental variability and intense extreme climatic events show more fragmented distribution patterns. In contrast, habitats with stable environmental conditions and lower intensity of extremes generally exhibit lower interannual dispersal levels, characterized by more concentrated distribution and longer reuse duration. Areas with longer reuse periods indicate habitat preferences of emperor penguins, and may demonstrate areas of ecological significance for breeding success. Annual habitat dispersal distance also shows sensitivity to the intensity of extreme events. Heat and blizzard events enhance dispersal distance, while wind and SIC exhibit primarily non-monotonic effects. These findings indicate that emperor penguins possess the ability to assess habitat quality and can adapt to harsh environments by flexibly relocating to more suitable breeding sites (Ainley et al., 2010). However, with increasing extreme events (Pörtner and Roberts, 2022) and their compound effects, the effectiveness of these dispersal strategies and the stability of future emperor penguin breeding habitats may be compromised.

### 5.2. Environmental impacts

The impacts of temperature, snowfall, wind, and sea ice on emperor penguins and their breeding habitats are extensive and interconnected. Emperor penguins maintain a stable core body temperature by balancing heat loss to the environment with metabolic heat production, and large temperature fluctuations in their habitat can severely disrupt this thermal balance (Stonehouse, 1967). Moreover, warming causes snowmelt and reduces habitat quality, prompting penguins to relocate to areas with fresh snow (Kooyman et al., 1990). Blizzards pose a serious threat to breeding emperor penguins, including hindering adult foraging and causing chick mortality (Budd, 1961; Fraser et al., 2013). The non-monotonic response curves of wind and sea ice (Fig. 14d,f) reflect a general threshold effect on habitat food supply and safety, i.e., excessively high or low intensities of these factors can reduce habitat quality. When the prevailing wind is dominated by katabatic winds from the ice sheet, moderate wind speed helps maintain nearby polynyas, providing favorable foraging grounds (Stonehouse, 1967). If wind speed is too low, accompanied by high SIC, it becomes difficult to maintain these foraging grounds. Conversely, strong winds can destabilize fast ice and diminish habitat safety (Ainley et al., 2010). Previous studies report that storms carved deep gullies into the relatively sheltered habitat of the Auster Islands and caused many emperor penguins to fall and die in these areas (Budd, 1961). When prevailing winds are moist northerlies, strong winds can inhibit sea ice expansion, increase SIC, and reduce open water areas (Massom et al., 2006). These warm and humid winds can trigger blizzards, and the subsequent snowmelt poses significant threats to breeding habitats. For example, in 2001, a warm and moist air intrusion

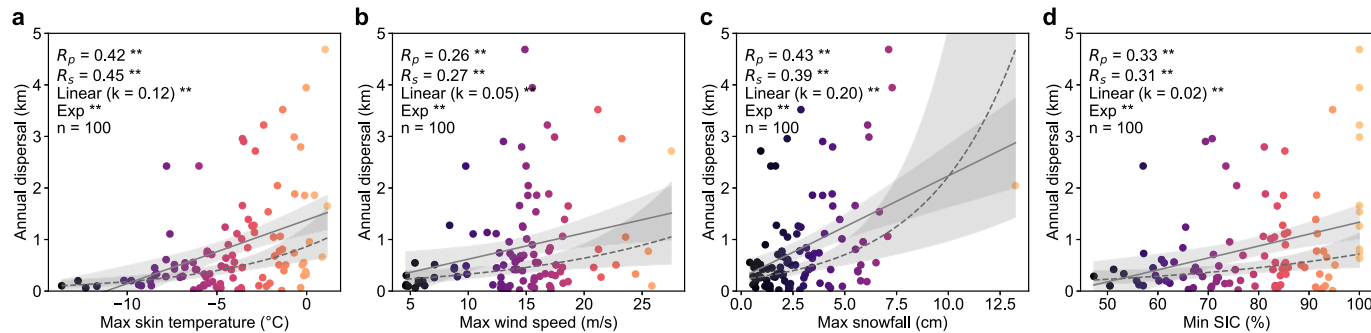


**Fig. 12.** Sensitivity of annual habitat dispersal distance to the intensities of extreme climatic events, including heat (a), storm (b), blizzard (c), and low sea ice (d). Pearson correlation coefficient ( $R_p$ ) and Spearman correlation coefficient ( $R_s$ ) between extreme events and annual dispersal distance are shown in each subplot. Linear and exponential regressions are used to fit the data. \*\* denotes  $P < 0.05$ .

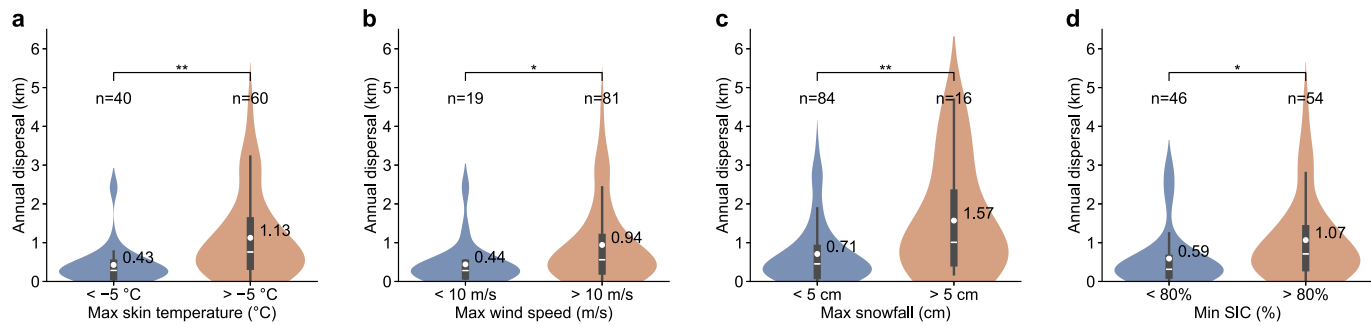


**Fig. 13.** Responses of annual habitat dispersal distance to varying intensities of extreme climatic events. Max daily skin temperature (a), max daily wind speed (b), total snowfall over the five snowiest consecutive days (c), and min daily SIC (d) are grouped using thresholds of 5 °C, 10 m/s, 5 cm, and 80 %, respectively. Violin plots display the mean (white dot, with values labeled nearby), median (white line), 25th and 75th percentiles, and whiskers representing the range within 1.5 times the interquartile range from the upper and lower quartiles. Two-tailed permutation tests were conducted to assess whether annual dispersal distances differ significantly between groups. \* and \*\* denote  $0.05 < P < 0.1$  and  $P < 0.05$ , respectively.

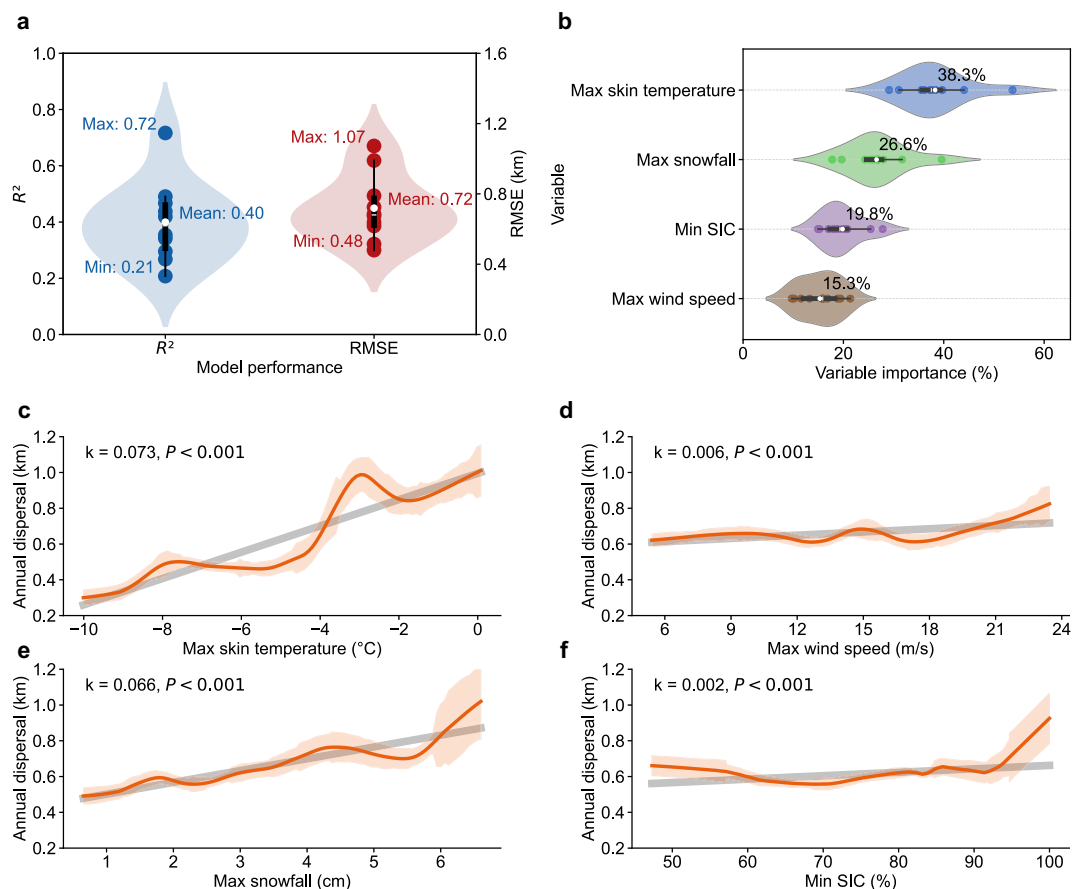


**Fig. 14.** Habitat dispersal model for emperor penguins. a, Model performance. The model was trained 10 times using a bootstrap method, and the coefficient of determination ( $R^2$ ) and root mean squared error (RMSE) values from all iterations are displayed. In the violin plots, the white dot indicates the mean, and the white line represents the median. b, Predictor importance derived from the 10 iterations. The violin plot structure is consistent with a, with text annotations indicating the mean values. c-f, Response of annual habitat dispersal distance to individual extreme climatic events, including heat (c), storm (d), blizzard (e), and low sea ice (f). The orange line represents the mean ensemble of 10 iterations, smoothed using loess, with shading indicating  $\pm 1$  standard deviation. The grey line indicates the linear regression fit.

over the southwestern Antarctic Peninsula resulted in heavy snowfall. The subsequent meltwater flooded Adélie penguin nests, leading to the drowning of numerous chicks (Massom et al., 2006). Compared to Adélie penguins, emperor penguins are not restricted by nests and can adjust their positions during blizzard events to find more suitable breeding areas (Stonehouse, 1953). However, under excessively harsh conditions, adult penguins may abandon breeding sites prematurely (Budd, 1961).

During the study period, fast ice at most habitats remained stable, allowing emperor penguins to adjust their positions in response to environmental changes. For instance, in 2014, when Cape Colbeck experienced higher temperature and snowfall along with a significant reduction in SIC, the colony relocated to a more sheltered area (Fig. S8). However, when extreme events become excessively severe, penguins may lose the capacity to adapt. Between 2022 and 2023, under record-low Antarctic sea ice conditions, the fast ice at Smiley broke up

prematurely. Emperor penguins were forced to temporarily shelter on nearby grounded icebergs (Fig. 15), ending in complete breeding failure (Fretwell et al., 2023). The number of colonies affected by early sea-ice loss has been increasing in recent years (Fretwell, 2024). Substantial sea ice loss can further enhance ocean-atmosphere interactions and increase storms (Josey et al., 2024). Under the intensification of future extreme climatic events (Pörtner and Roberts, 2022), emperor penguins may move longer distances to find suitable breeding areas, but only if sheltered terrain and stable fast ice are available.

### 5.3. Implications for the SDGs and future prospects

SDG Goal 13 emphasizes the need to take urgent action to address climate change and its impacts. Climate models project future surface warming over Antarctica under the low-emission scenario (Shared Socioeconomic Pathway (SSP) 1–2.6) and high-emission scenario (SSP5–8.5) to be 1.3 °C and 4.8 °C, respectively (Bracegirdle et al., 2020). Applying these projections to the sensitivity of emperor penguin annual habitat dispersal to temperature (73 m/°C) gives a projected increase of 95–350 m by the end of the 21st century. Compared to the low-emission scenario using clean energy, the high-emission scenario driven by fossil fuels (Riahi et al., 2017) would result in an additional 255 m of annual habitat fragmentation. This result suggests that the stability of emperor penguin habitats would benefit from climate mitigation actions and global climate policy implementation (Jenouvrier et al., 2021) under SDG 13.

SDG Goal 14 and Goal 15 highlight the protection of marine and terrestrial ecosystems, respectively. Penguins are key biological pumps in the Antarctic ecosystem, and they transport nutrients such as nitrogen and phosphorus from the ocean to land through their guano (Otero et al., 2018). A recent study indicates that penguin colonies act as local hot-spots of nutrients and stimulate primary productivity, while a significant decline in penguin populations could have profound impacts on surrounding ecosystems (Belyaev et al., 2023). The automated habitat mapping method provides an innovative tool for monitoring and protecting coastal ecosystems under Target 14.2. Our satellite-based assessment of habitat degradation contributes to the evaluation of SDG indicator 15.5.1, the Red List Index, and the Biodiversity Risk Index

(Guo et al., 2022).

By incorporating additional spectral bands, our approach can be extended to future Sustainable Development Satellite Constellation (Guo et al., 2025) to achieve routine monitoring and regular update of emperor penguin habitat use and contribute to global SDGs monitoring and assessment.

Major factors influencing emperor penguin breeding habitats include microclimate, food availability, and safety (Budd, 1961). The portion of variation unexplained by extreme climatic events may be driven by factors more directly related to food distribution (e.g., fish and krill) and habitat safety (e.g., geomorphological features, grounded icebergs, and fast ice thickness). The relation between habitat dispersal and sheltered terrain or food availability warrants further investigation, particularly with increasing iceberg calving (Qi et al., 2021) and future changes in prey distribution in the Southern Ocean (Hindell et al., 2020). Regular mapping and updating of emperor penguin habitat distribution, combined with a monitoring network linking field and satellite observations, will be essential for predicting the future habitat use and survival prospects of emperor penguins.

### 5.4. Limitations

Substantial cloud contamination in the Antarctic coastal region (Fraser et al., 2009) poses challenges for mapping emperor penguin habitats. During the study period, the mean number of usable Landsat 8 images from September to November each year was 10 (Fig. 4). Our composite images integrated habitat distribution information from individual images, partially mitigating the issues of guano signal loss due to cloud contamination and intra-annual habitat location variability. Snowfall can also obscure guano signals (Ancel et al., 2014). However, the habitat dispersal analysis framework is based on habitat centroids, making it robust to localized signal loss. We acknowledge that our habitat detection method produces false positives in some rocky regions, but these errors are minimal. When necessary, we manually corrected a small number of misclassified images (Supplementary Materials). In addition, the random forest model used in this study classifies based on pixel-level features and makes limited use of spatial structural characteristics, such as the distinctive morphology of emperor penguin

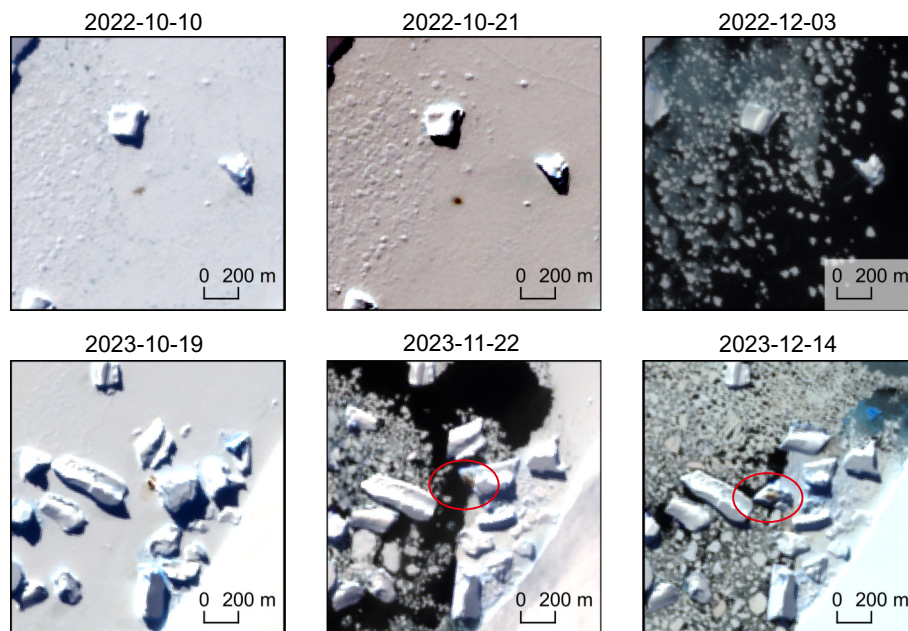


**Fig. 15.** Habitat loss at Smiley caused by premature fast ice breakup between 2022 and 2023. Red circles indicate emperor penguins taking shelter on nearby icebergs after the breakup of fast ice. The base maps are Sentinel-2 images with similar characteristics as Landsat. (For interpretation of the references to colour in this figure legend, the reader is referred to the web version of this article.)

colonies. The proposed method may face challenges in mapping penguin colonies with fewer than 1000 pairs due to the limited spatial resolution of Landsat imagery. Due to illumination constraints, optical remote sensing imagery cannot effectively capture emperor penguin habitat information before September (Winterl et al., 2024). This limitation results in the absence of early breeding season dynamics from the analysis.

We also observed that Adélie penguin colonies exhibit high values in the guano index maps. However, the rocky regions where Adélie penguins typically nest were masked out in data pre-processing to mitigate the impacts of background rock signals on the detection of emperor penguin colonies. This limitation results in the absence of early breeding season dynamics from the analysis.

## 6. Conclusions

This study developed a novel and automated method for detecting emperor penguin habitats using Landsat 8 satellite imagery, enabling the monitoring of habitat dynamics across large spatial scales. We mapped the annual habitat distribution of 10 important emperor penguin colonies from 2013 to 2023 and generated habitat use maps. By integrating climate data, we found that habitats with greater climate variability and stronger extreme events exhibited more fragmented distributions and shorter occupancy durations. At the annual scale, we observed a positive correlation between the intensity of heat, blizzard, storm, and low sea ice events and the annual dispersal distance. These extreme events collectively explained 21 %–72 % of the variance in annual habitat dispersal. Given the complex environment of Antarctica, even short-distance dispersal may have significant impacts, as newly occupied sites with increased exposure to strong winds, lack of shelter, or poor foraging conditions may lead penguins into ecological traps (Fretwell et al., 2014; Robertson and Hutto, 2006). These findings underline the significant impact of extreme events on emperor penguin habitat dispersal and use patterns, suggesting that adopting sustainable global climate policies will be essential to mitigate future habitat fragmentation.

The satellite-based monitoring framework developed in this study provides a repeatable, and long-term approach for tracking the ecological consequences of climate change in remote polar ecosystems. By delivering spatially explicit evidence of climate-driven habitat fragmentation, this research supports climate adaptation strategies, biodiversity conservation, and sustainable ecosystem governance. Moreover, it demonstrates the critical role of remote sensing technologies in advancing global environmental monitoring and informing science-based policy decisions (Zhao and Yu, 2025). Our study on climate-driven habitat changes in Antarctica contributes to the advancement of the broader SDGs related to marine and terrestrial ecosystem conservation.

## CRediT authorship contribution statement

**Hong Lin:** Writing – review & editing, Writing – original draft, Visualization, Validation, Software, Methodology, Investigation, Formal analysis, Data curation, Conceptualization. **Xiao Cheng:** Writing – review & editing, Supervision, Resources, Project administration, Methodology, Funding acquisition, Formal analysis, Conceptualization. **Jinyang Du:** Writing – review & editing, Supervision, Resources, Project administration, Methodology, Formal analysis, Conceptualization. **John S. Kimball:** Writing – review & editing, Supervision, Resources, Project administration, Methodology, Formal analysis, Conceptualization. **Ziyu Yan:** Validation, Methodology, Investigation, Data curation. **Teng Li:** Supervision, Project administration, Methodology, Funding acquisition, Conceptualization. **Tongwen Li:** Supervision, Methodology, Conceptualization. **Yibo Li:** Validation, Software, Data curation. **Zilong Chen:** Validation, Software, Data curation.

## Declaration of competing interest

The authors declare that they have no known competing financial interests or personal relationships that could have appeared to influence the work reported in this paper.

## Acknowledgements

This work was supported by the National Key Research and Development Program of China (Grant No. 2024YFC2813601) and the National Natural Science Foundation of China (No. 42206249). The authors sincerely appreciate the insightful comments from the reviewers, which have greatly improved this article.

## Appendix A. Supplementary data

Supplementary data to this article can be found online at <https://doi.org/10.1016/j.rse.2025.114984>.

## Data availability

Data used in this study are available as follows: Landsat 8, <https://www.usgs.gov/landsat-missions/landsat-collection-2-level-2-science-products>; ERA5-Land, <https://cds.climate.copernicus.eu/datasets/derived-era5-land-daily-statistics?tab=download>; PFV53, [https://www.ncei.noaa.gov/access/metadata/landing-page/bin/iso?id=gov.noaa.ncdc:AVHRR\\_Pathfinder-NCEI-L3C-v5.3](https://www.ncei.noaa.gov/access/metadata/landing-page/bin/iso?id=gov.noaa.ncdc:AVHRR_Pathfinder-NCEI-L3C-v5.3). Associated code is available at <https://doi.org/10.5281/zenodo.13370904>.

## References

- Ainley, D., Russell, J., Jenouvrier, S., Woehler, E., Lyver, P.O., Fraser, W.R., Kooyman, G.L., 2010. Antarctic penguin response to habitat change as earth's troposphere reaches 2°C above preindustrial levels. *Ecol. Monogr.* 80, 49–66.
- Ancel, A., Cristofari, R., Fretwell, P.T., Trathan, P.N., Wienecke, B., Boureau, M., Morinay, J., Blanc, S., Le Maho, Y., Le Bohec, C., 2014. Emperors in hiding: when ice-breakers and satellites complement each other in Antarctic exploration. *PLoS One* 9.
- Barbraud, C., Weimerskirch, H., 2001. Emperor penguins and climate change. *Nature* 411, 183–186.
- Bartlett, M.S., 1947. The use of transformations. *Biometrics* 3, 39–52.
- Belgiu, M., Drăguț, L., 2016. Random forest in remote sensing: a review of applications and future directions. *ISPRS J. Photogramm. Remote Sens.* 114, 24–31.
- Belyaev, O., Sparaventi, E., Navarro, G., Rodríguez-Romero, A., Tovar-Sánchez, A., 2023. The contribution of penguin guano to the Southern Ocean iron pool. *Nat. Commun.* 14, 1781.
- Bracegirdle, T.J., Krinner, G., Tonelli, M., Haumann, F.A., Naughten, K.A., Rackow, T., Roach, L.A., Wainer, I., 2020. Twenty first century changes in Antarctic and Southern Ocean surface climate in CMIP6. *Atmos. Sci. Lett.* 21, e984.
- Breiman, L., 2001. Random forests. *Mach. Learn.* 45, 5–32.
- Budd, G.M., 1961. The biotopes of emperor penguin rookeries. *Emu-Austral Ornithol.* 61, 171–189.
- Budd, G.M., 1962. Population studies in rookeries of the emperor penguin *Aptenodytes forsteri*. *Proc. Zool. Soc. London* 139, 365–388.
- Burton-Johnson, A., Black, M., Fretwell, P.T., Kaluza-Gilbert, J., 2016. An automated methodology for differentiating rock from snow, clouds and sea in Antarctica from Landsat 8 imagery: a new rock outcrop map and area estimation for the entire Antarctic continent. *Cryosph* 10, 1665–1677.
- Cristofari, R., Bertorelle, G., Ancel, A., Benazzo, A., Le Maho, Y., Ponganis, P.J., Stenseth, N.C., Trathan, P.N., Whittington, J.D., Zanetti, E., 2016. Full circumpolar migration ensures evolutionary unity in the emperor penguin. *Nat. Commun.* 7, 11842.
- Croxall, J.P., Trathan, P.N., Murphy, E., 2002. Environmental change and Antarctic seabird populations. *Science* 297, 1510–1514.
- Dugger, K.M., Ainley, D.G., Lyver, P.O., Barton, K., Ballard, G., 2010. Survival differences and the effect of environmental instability on breeding dispersal in an Adélie penguin meta-population. *Proc. Natl. Acad. Sci.* 107, 12375–12380.
- Forcada, J., Trathan, P.N., 2009. Penguin responses to climate change in the Southern Ocean. *Glob. Chang. Biol.* 15, 1618–1630.
- Fraser, A.D., Massom, R.A., Michael, K.J., 2009. A method for compositing polar MODIS satellite images to remove cloud cover for landfast sea-ice detection. *IEEE Trans. Geosci. Remote Sens.* 47, 3272–3282.
- Fraser, W.R., Patterson-Fraser, D.L., Ribic, C.A., Schofield, O., Ducklow, H., 2013. A nonmarine source of variability in Adélie penguin demography. *Oceanography* 26, 207–209.
- Fretwell, P.T., 2024. A 6 year assessment of low sea-ice impacts on emperor penguins. *Antarct. Sci.* 36, 3–5.

- Fretwell, P.T., Trathan, P.N., 2009. Penguins from space: faecal stains reveal the location of emperor penguin colonies. *Glob. Ecol. Biogeogr.* 18, 543–552.
- Fretwell, P.T., LaRue, M.A., Morin, P., Kooyman, G.L., Wienecke, B., Ratcliffe, N., Fox, A.J., Fleming, A.H., Porter, C., Trathan, P.N., 2012. An emperor penguin population estimate: the first global, synoptic survey of a species from space. *PLoS One* 7.
- Fretwell, P.T., Trathan, P.N., Wienecke, B., Kooyman, G.L., 2014. Emperor penguins breeding on ice shelves. *PLoS One* 9.
- Fretwell, P.T., Phillips, R.A., Brooke, M.L., Fleming, A.H., McArthur, A., 2015. Using the unique spectral signature of guano to identify unknown seabird colonies. *Remote Sens. Environ.* 156, 448–456.
- Fretwell, P.T., Bouet, A., Ratcliffe, N., 2023. Record low 2022 Antarctic Sea ice led to catastrophic breeding failure of emperor penguins. *Commun. Earth Environ.* 4, 273.
- Guo, H., Liang, D., Sun, Z., Chen, F., Wang, X., Li, J., Zhu, L., Bian, J., Wei, Y., Huang, L., 2022. Measuring and evaluating SDG indicators with big earth data. *Sci. Bull.* 67, 1792–1801.
- Guo, H., Dou, C., Liang, D., Fu, B., Chen, H., Zou, Z., Huang, P., Li, X., Chen, F., Han, C., Jing, J., Hu, T., Yan, L., Hu, Y., Tang, Y., Jiang, N., Feng, X., Ding, H., Zhang, H., Qiao, E., Zhou, B., 2025. The SDGSAT-1 mission and its role in monitoring SDG indicators. *Remote Sens. Environ.* 328, 114885.
- Hák, T., Janoušková, S., Moldan, B., 2016. Sustainable development goals: a need for relevant indicators. *Ecol. Indic.* 60, 565–573.
- Hindell, M.A., Reisinger, R.R., Ropert-Coudert, Y., Hückstädt, L.A., Trathan, P.N., Bornemann, H., Charrassin, J.-B., Chown, S.L., Costa, D.P., Danis, B., 2020. Tracking of marine predators to protect Southern Ocean ecosystems. *Nature* 580, 87–92.
- Humphries, G.R.W., Naveen, R., Schwaller, M., Che-Castaldo, C., McDowall, P., Schrimpf, M., Lynch, H.J., 2017. Mapping application for penguin populations and projected dynamics (MAPPPD): data and tools for dynamic management and decision support. *Polar Rec.* 53, 160–166.
- IUCN, 2024. IUCN Red List of Threatened Species. Version 2020. Available. [www.iucnredlist.org](http://www.iucnredlist.org). Accessed on 12 December 2024.
- Jenouvrier, S., Holland, M., Stroeve, J., Serreze, M., Barbraud, C., Weimerskirch, H., Caswell, H., 2014. Projected continent-wide declines of the emperor penguin under climate change. *Nat. Clim. Chang.* 4, 715–718.
- Jenouvrier, S., Judy, C.C., Wolf, S., Holland, M., Labrousse, S., LaRue, M., Wienecke, B., Fretwell, P., Barbraud, C., Greenwald, N., Stroeve, J., Trathan, P.N., 2021. The call of the emperor penguin: legal responses to species threatened by climate change. *Glob. Chang. Biol.* 27, 5008–5029.
- Josey, S.A., Meijers, A.J.S., Blaker, A.T., Grist, J.P., Mecking, J., Ayres, H.C., 2024. Record-low Antarctic Sea ice in 2023 increased ocean heat loss and storms. *Nature* 636, 635–639.
- Kooyman, G.L., 1993. Breeding habitats of emperor penguins in the western Ross Sea. *Antarct. Sci.* 5, 143–148.
- Kooyman, G.L., Ponganis, P.J., 2017. Rise and fall of Ross Sea emperor penguin colony populations: 2000 to 2012. *Antarct. Sci.* 29, 201–208.
- Kooyman, G.L., Croll, D., Stone, S., Smith, S., 1990. Emperor penguin colony at Cape Washington, Antarctica. *Polar Rec.* 26, 103–108.
- Kooyman, G.L., Ainley, D.G., Ballard, G., Ponganis, P.J., 2007. Effects of giant icebergs on two emperor penguin colonies in the Ross Sea, Antarctica. *Antarct. Sci.* 19, 31–38.
- Labrousse, S., Nerini, D., Fraser, A.D., Salas, L., Sumner, M., Le Manach, F., Jenouvrier, S., Iles, D., LaRue, M., 2023. Where to live? Landfast Sea ice shapes emperor penguin habitat around Antarctica. *Sci. Adv.* 9, eadg8340.
- LaRue, M.A., Kooyman, G., Lynch, H.J., Fretwell, P., 2015. Emigration in emperor penguins: implications for interpretation of long-term studies. *Ecography* 38, 114–120.
- LaRue, M., Iles, D., Labrousse, S., Fretwell, P., Ortega, D., Devane, E., Horstmann, I., Viollat, L., Foster-Dyer, R., Le Bohec, C., 2024. Advances in remote sensing of emperor penguins: first multi-year time series documenting trends in the global population. *Proc. R. Soc. B* 291, 20232067.
- Lescroël, A., Ballard, G., Grémillet, D., Authier, M., Ainley, D.G., 2014. Antarctic climate change: extreme events disrupt plastic phenotypic response in Adélie penguins. *PLoS One* 9, e85291.
- Li, Xin, Guo, H., Cheng, G., Song, X., Ran, Y., Feng, M., Che, T., Li, Xinwu, Wang, L., Duan, A., 2025. Polar regions are critical in achieving global sustainable development goals. *Nat. Commun.* 16, 3879.
- Massom, R.A., Stammerjohn, S.E., Smith, R.C., Pook, M.J., Iannuzzi, R.A., Adams, N., Martinson, D.G., Vernet, M., Fraser, W.R., Quetin, L.B., 2006. Extreme anomalous atmospheric circulation in the West Antarctic peninsula region in austral spring and summer 2001/02, and its profound impact on sea ice and biota. *J. Clim.* 19, 3544–3571.
- Maxwell, A.E., Warner, T.A., Fang, F., 2018. Implementation of machine-learning classification in remote sensing: an applied review. *Int. J. Remote Sens.* 39, 2784–2817.
- Muñoz-Sabater, J., Dutra, E., Agustí-Panareda, A., Albergel, C., Arduini, G., Balsamo, G., Boussetta, S., Choulga, M., Harrigan, S., Hersbach, H., 2021. ERA5-land: a state-of-the-art global reanalysis dataset for land applications. *Earth Syst. Sci. Data* 13, 4349–4383.
- Osborne, J., 2010. Improving your data transformations: Applying the Box-Cox transformation. *Pract. Assess. Res. Eval.* 15.
- Otero, X.L., De La Peña-Lastra, S., Pérez-Alberti, A., Ferreira, T.O., Huerta-Díaz, M.A., 2018. Seabird colonies as important global drivers in the nitrogen and phosphorus cycles. *Nat. Commun.* 9, 246.
- Pörtner, H.-O., Roberts, D.C., 2022. Climate Change 2022: Impacts, Adaptation and Vulnerability.
- Qi, M., Liu, Y., Liu, J., Cheng, X., Lin, Y., Feng, Q., Shen, Q., Yu, Z., 2021. A 15-year circum-Antarctic iceberg calving dataset derived from continuous satellite observations. *Earth Syst. Sci. Data* 13, 4583–4601.
- Riahi, K., Van Vuuren, D.P., Kriegler, E., Edmonds, J., O'Neill, B.C., Fujimori, S., Bauer, N., Calvin, K., Dellink, R., Fricko, O., 2017. The shared socioeconomic pathways and their energy, land use, and greenhouse gas emissions implications: an overview. *Glob. Environ. Chang.* 42, 153–168.
- Robertson, B.A., Hutto, R.L., 2006. A framework for understanding ecological traps and an evaluation of existing evidence. *Ecology* 87, 1075–1085.
- Saha, K., Zhao, X., Zhang, H.M., Casey, K.S., Zhang, D., Baker-Yeboah, S., Kilpatrick, K.A., Evans, R.H., Ryan, T., Relph, J.M., 2018. AVHRR pathfinder version 5.3 level 3 collated (L3C). In: Global 4km Sea Surface Temperature for 1981–Present. NOAA Natl. Centers Environ. Inf. Asheville, NC, USA.
- Schwaller, M.R., Southwell, C.J., Emmerson, L.M., 2013. Continental-scale mapping of Adélie penguin colonies from Landsat imagery. *Remote Sens. Environ.* 139, 353–364.
- Sillmann, J., Kharin, V.V., Zhang, X., Zwiers, F.W., Branaugh, D., 2013. Climate extremes indices in the CMIP5 multimodel ensemble: part 1. Model evaluation in the present climate. *J. Geophys. Res. Atmos.* 118, 1716–1733.
- Stonehouse, B., 1953. The Emperor Penguin (*Aptenodytes forsteri*, Gray): I. Breeding Behaviour and Development.
- Stonehouse, B., 1967. The general biology and thermal balances of penguins. *Adv. Ecol. Res.* 4, 131–196.
- Trathan, P.N., Fretwell, P.T., Stonehouse, B., 2011. First recorded loss of an emperor penguin colony in the recent period of Antarctic regional warming: implications for other colonies. *PLoS One* 6, e14738.
- Trathan, P.N., Wienecke, B., Barbraud, C., Jenouvrier, S., Kooyman, G., Le Bohec, C., Ainley, D.G., Ancel, A., Zitterbart, D.P., Chown, S.L., 2020. The emperor penguin vulnerable to projected rates of warming and sea ice loss. *Biol. Conserv.* 241, 108216.
- Wang, Y., Hollingsworth, P.M., Zhai, D., West, C.D., Green, J.M.H., Chen, H., Hurni, K., Su, Y., Warren-Thomas, E., Xu, J., 2023. High-resolution maps show that rubber causes substantial deforestation. *Nature* 623, 340–346.
- Winterl, A., Richter, S., Houstin, A., Barracho, T., Boureau, M., Corne, C., Couet, D., Cristofari, R., Eiselt, C., Fabry, B., 2024. Remote sensing of emperor penguin abundance and breeding success. *Nat. Commun.* 15, 4419.
- Zhao, Q., Yu, L., 2025. Advancing sustainable development goals through earth observation satellite data: current insights and future directions. *J. Remote Sens.* 5, 403.